Inverse scattering for shape and conductivity

Wei Chien and Chien Ching Chiu

Electrical Engineering Department, Tamkang University

Tamsui, Taipei, China

Chiu@ee.tku.edu.tw

Abstract

We consider the inverse problem of determining both the shape and the conductivity of a two-dimensional conducting scatterer from a knowledge of the far-field pattern of TM waves by solving the ill posed nonlinear equation. Based on the boundary condition and the measured scattered field, a set of nonlinear integral equations is derived and the imaging problem is reformulated into an optimization problem. Satisfactory reconstructions have been achieved by the genetic algorithm. Numerical results demonstrated that, even when the initial guess is far away from the exact one, good reconstruction has been obtained. Numerical results show that multiple incident directions permit good reconstruction of shape and conductivity.

I. INTRODUCTION

This paper deals with the question of determining both the shape and the variable conductivity from a knowledge of the far-field pattern of the scattered wave for a set of incident TM waves.

The usual inverse obstacle scattering problem is to determine the shape of the obstacle given information about the far-field pattern of the scattered wave from each of a set of incident fields. We are asking in addition to recover the conductivities of the obstacle, given these are of variable conductivity type. Carrying this idea further, we can ask if it is possible, by modifying the conductivity values of the boundary of an obstacle, to make it appear from a scattering experiment standpoint as some object of a different shape.

In this paper, the electromagnetic imaging of a variable conducting cylinder in free space is investigated. The genetic algorithm [1] is used to recover not only the shape but also the conductivity of a scatterer, by using only the scattered field. The method is potentially important in medical imaging and biological application. In Section II, a theoretical formulation for the electromagnetic imaging is presented. The general principle of genetic algorithms and the way we applied them to the imaging problem are described. Numerical results for objects of different shapes and conductivities are given in Section III. Finally, some conclusions are drawn in Section IV.

II. THEORETICAL FORMULATION

Let us consider an imperfectly conducting cylinder with conductivity $\sigma(\theta)$ in free space. The metallic cylinder with cross section described in polar coordinates in xy plane by the equation $\rho = F(\theta)$ is

0-7803-7831-8/03/$17.00

illuminated by transverse magnetic (TM) waves. We assume that time dependence of the field is harmonic with the factor exp($j\omega t$). Let $\bar{E}_i$ denote the incident field with incident angle ϕ, shown in Fig. 1.

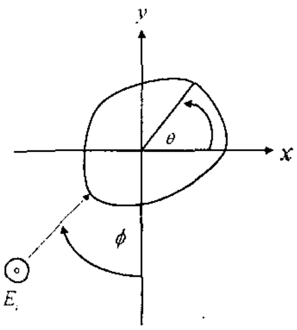

Fig. 1 Geometry of the problem in (x,y) plane

Then the incident field is given by

$$\vec{E}_i(x,y) = e^{-jk(x\sin\phi + y\cos\phi)}\hat{z}\ ,\ \ k^2 = \omega^2\varepsilon_0\mu_0 \qquad (1)$$

At an arbitrary point (x, y) in Cartesian coordinates or (r,θ) in polar coordinates outside the scattered field, $\bar{E}_s = \bar{E} - \bar{E}_i$ can be expressed by

$$E_s(x,y) = -\int_0^{2\pi} \frac{j}{4} H_0^{(2)} \cdot (k\sqrt{(x-F(\theta)\cos\theta)^2 + (y-F(\theta)\sin\theta)^2})J(\theta)d\theta \qquad (2)$$

with $J(\theta) = -j\omega\mu_0\sqrt{F^2(\theta)+F'^2(\theta)}J_s(\theta)$, $H_0^{(2)}$ is the Hankel function of second kind of order zero, and $J_s(\theta)$ is the induced surface current density.

The boundary condition for an imperfectly conducting scatterer with finite conductivity can be approximated by assuming that the total tangential electric field on the scatterer surface is related to surface current density through a surface impedance $Z_s(\omega)$:

$$\hat{n} \times \bar{E} = \hat{n} \times (Z_s \bar{J}_s) \qquad (3)$$

where $\hat{n}$ is the outward unit vector normal to the surface of the scatterer. The surface impedance is expressed in [2] as $Z_s(\omega,\theta) \cong \sqrt{j\omega\mu_0/\sigma(\theta)}$. The boundary condition at the surface of the scatterer given by (3) then yield an integral equation for $J(\theta)$:

$$E_i(F(\theta),\theta) = \int_0^{2\pi} \frac{j}{4} H_0^{(2)}(kr_0)J(\theta')d\theta' + j\sqrt{\frac{j}{\omega\mu_0\sigma(\theta)}}\frac{J(\theta)}{\sqrt{F^2(\theta)+F'^2(\theta)}} \qquad (4)$$

where

$$r_0(\theta,\theta') = [F^2(\theta) + F^2(\theta') - 2F(\theta)F(\theta')\cos(\theta-\theta')]^{1/2}$$

For the direct scattering problem, the scattered field, E_s, is calculated by assuming that the shape and the conductivity of the object are known. This can be achieved by first solving J in (4) and calculating E_s in (2). Let us consider the following inverse problem, the shape function $F(\theta)$ and conductivity function $\sigma(\theta)$ can be expanded as:

$$F(\theta) = \sum_0^{N/2} B_n \cos(n\theta) + \sum_{n=1}^{N/2} C_n \sin(n\theta) \qquad (5)$$

$$\sigma(\theta) = \sum_{m=0}^{M/2} D_m \cos(m\theta) + \sum_{m=1}^{M/2} E_m \sin(m\theta)$$

where B_n, C_n, D_m and E_m are real coefficient to be determined, and (N+1)+(M+1) is the number of unknowns for shape function and conductivity function. The genetic algorithm is used to minimize the following cost function:

$$CF = \left\{ \frac{1}{Z_t} \sum_{z=1}^{Z_t} \left| E_s^{\exp}(\bar{r}_z) - E_s^{cal}(\bar{r}_z) \right|^2 \Big/ \left| E_s^{\exp}(\bar{r}_z) \right|^2 + \alpha \left| F'(\theta) \right|^2 \right\}^{1/2} \qquad (7)$$

where Z_t is the total number of measured points. $E_s^{\exp}(\bar{r})$ and $E_s^{cal}(\bar{r})$ are the measured scattered field and the calculated scattered field respectively. The minimization of $\alpha|F'(\theta)|^2$ can, to a certain extent, be interpreted as the smoothness requirement for the boundary of $F(\theta)$. The basic GA for which a flowchart is shown in Fig. 2 starts with a large population containing a total of X candidates. Each candidate is described by a chromosome. Then the initial population can simply be created by taking X random chromosomes. Finally, the GA iteratively generates a new population which is derived from the previous population through the application of the reproduction, crossover, and mutation operators.

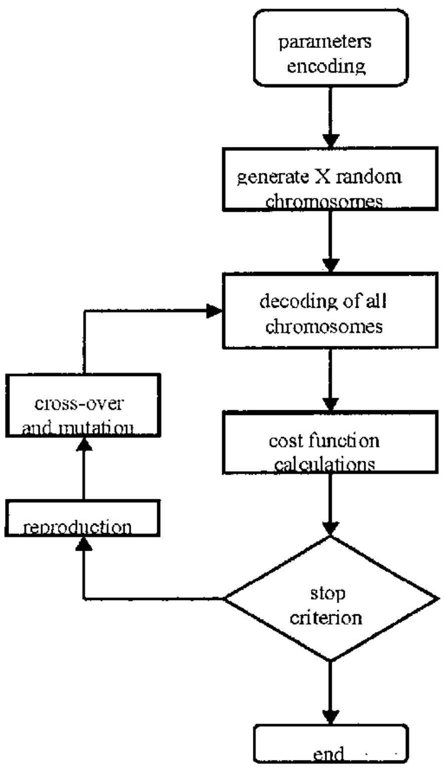

Fig. 2 The flowchart of GA

III. NUMERICAL RESULTS

By a numerical simulation we illustrate the performance of the proposed inversion algorithm. The frequency of the incident wave is chosen to be 3 GHz; i.e., the wavelength λ is 0.1 m. In the example, the size of the scatterer is about one third the wavelength, so the frequency is in the resonance range. The shape and conductivity function are chosen to be:

$$F(\theta) = (0.03 + 0.005\cos\theta + 0.009\cos 2\theta)\,\text{m and}$$

$$\sigma(\theta) = (80 + 12\cos\theta + 15\cos 2\theta + 10\sin\theta + 18\sin 2\theta)\ \text{S/m}.$$

The reconstructed shape and conductivity function for the best population member are plotted in Fig. 3(a) and Fig. 3(b) with the error shown in Fig. 3(c), where DR and DSIG are called shape function and conductivity discrepancies respectively.

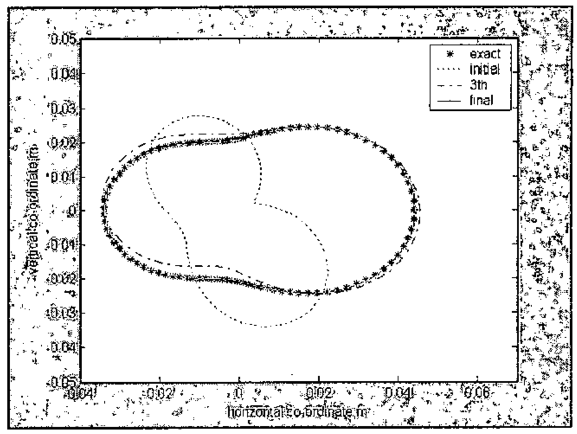

Fig. 3(a) Shape function. The star curve represents the exact shape , while the solid curves are calculated shape in iteration process.

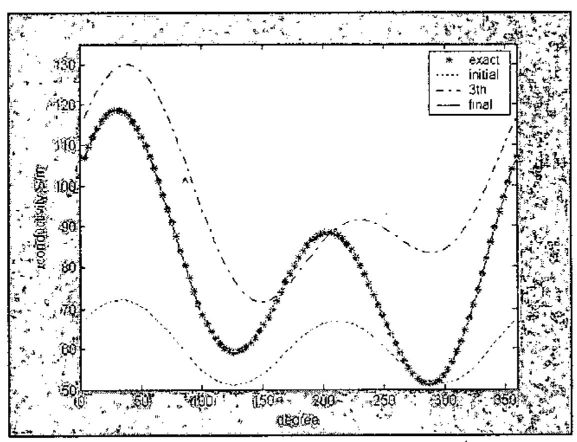

Fig. 3(b) Conductivity function. The star curve represents the exact conductivity, while the solid curves are calculated conductivity in iteration process.

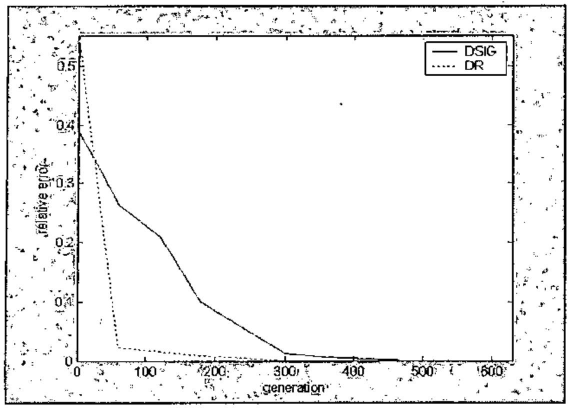

Fig. 3(c) Shape function error and conductivity function error

$$DR = \{\frac{1}{N'}\sum_{i=1}^{N'}[F^{cal}(\theta_i) - F(\theta_i)]^2 / F^2(\theta_i)\}^{1/2}$$

$$DSIG = \{\frac{1}{N'}\sum_{i=1}^{N'}[\sigma^{cal}(\theta_i) - \sigma(\theta_i)]^2 / \sigma^2(\theta_i)\}^{1/2}$$

where N' is set to 60. Quantities *DR* and *DSIG* provide measures of how well $F^{cal}(\theta)$ approximates $F(\theta)$ and $\sigma^{cal}(\theta)$ approximates $\sigma(\theta)$, respectively. From Fig. 3, it is clear that the reconstructions of the shape and conductivity function are quite good. In addition, we also see that the reconstruction of conductivity function does not change rapidly toward the exact Value until *DR* is small enough. This can be explained by the fact that the shape makes a stronger contribution to the scattered field than the conductivity function does. In other words, the reconstruction of the shape function has a higher priority than the reconstruction of the conductivity function.

IV. CONCLUSIONS

We have presented a study of applying the genetic algorithm to reconstruct the shape and conductivity of a metallic object through knowledge of scattered field. Based on the boundary condition and measured scattered field, we have derived a set of nonlinear integral equations and reformulated the imaging problem into an optimization problem. By using the genetic algorithm, the shape and conductivity of the object can be reconstructed. Even when the initial guess is far from exact, the genetic algorithm converges to a global extreme of the cost function, while the gradient-based methods often get stuck in a local extreme. Good reconstruction has been obtained from the scattered fields both with and without the additive Gaussian noise. Numerical results also illustrate that the conductivity is more sensitive to noise than the shape function is. According to our experience, the main difficulties in applying the genetic algorithm to this problem are how to choose the parameters, such as the population size (X), bit length of the string (L), crossover probability (p_c), and mutation probability (p_m). Different parameter sets will affect the speed of convergence as well as the computing time required. From the numerical simulation, it is concluded that a population size from 300 to 600, a string length from 8 to 16 bits, and p_c and p_m in the ranges of $0.7 < p_c < 0.9$ and $0.0005 < p_m < 0.05$ are suitable for imaging problems of this type.

V. REFERENCES

[1] G. P. Otto and W. C. Chew, "Microwave inverse scattering-local shape function imaging for improved resolution of strong scatterers," *IEEE Trans. Microwave Theory Tech.*, vol. 42, pp. 137-141, Jan. 1994.

[2] F. M. Tesche, "On the inclusion of loss in time domain solutions of electromagnetic interaction problems," *IEEE Trans. Electromagn. Compat.*, vol. EMC-32, pp. 1-4, Feb. 1990.